Crack paths propagation under Mode II fracture in concrete composites containing fly-ash additive

G. L. Golewski[1] , P. Golewski[2] and T. Sadowski[2]

[1] Department of Civil Engineering Structures, Faculty of Civil Engineering and Architecture, Lublin University of Technology, Nadbystrzycka 40 str., 20-618 Lublin, Poland, glgol@wp.pl,
[2] Department of Solid Mechanics, Faculty of Civil Engineering and Architecture, Lublin University of Technology, Nadbystrzycka 40 str., 20-618 Lublin, Poland, t.sadowski@pollub.pl

ABSTRACT. *Siliceous fly-ash (FA) is one of the additive that are most frequently used for modification of concrete. FA is a valuable and necessary raw material for the building materials industry. Description of concretes behaviour under compression with many complex shaped cracks can be done by application of micromechanical model. During the material deformation cracks propagate under mixed-mode of fracture. Therefore it is necessary to estimate experimentally mode I and II of fracture toughness. The aim of this paper is an experimental and numerical analysis of crack paths propagation under Mode II fracture. This mode is important in the description of the concrete characterisation, due to relatively low shear strength and high sensitivity to the shear stress. Mode II fracture toughness of sharp notches and their development was carried out using specimens for two concrete mixtures: a) concrete without FA, b) concrete with 20% FA additive. Compact Shear Specimens (CSS) - 150x150x150 concrete cube with two sharp notches were used for tests under quasi-static loading using MTS testing machine and 3-D Image Correlation System.*
A new 3-D numerical model of the specimens for Mode II fracture was created with application XFEM. In calculations we used peak principal stress criterion for controlling crack propagation, taking into account the experimental data concerning strength parameters and fracture energy. The obtained results with the newly formulated 3-D numerical XFEM model coincide with experimental tests very well. Comparison of the crack shapes from both tests confirms correctness of assumptions made in the numerical model.

INTRODUCTION

One of the most frequently used additives to concrete is siliceous fly-ash (FA) which is a by-product of hard coal combustion process conducted in power plants and thermal-electric power stations [1]. Nowadays, good quality siliceous FA is used for production of plain concretes [2] as well as high performance concretes [3], self-compacting

concretes [3] or roller-compacted concretes [4]. A wide range of applications of composites modified with FA addition is connected also with high resistance to corrosion [5].
Destruction of brittle materials (e.g. concretes, ceramics) is a multi-stage process that is conditioned by value and type of applied external loads as well as internal structure of composite, e.g. [6 - 13]. According to [12], three below-specified characteristic points can be distinguished on the stress-strain diagram corresponding to different types of defects development in a concrete specimen subjected to compression stresses: 1st level of stress when straight defects (mesocrack) develop in the material, 2nd level of stress when wing defects start initiating at the ends of mesocrack, 3rd level of stress when a specimen is fragmented and destroyed as a result of unstable development of wing cracks. Thus, in the final stage of concrete element operation, just before its destruction, the time of destruction of the material is tightly connected with development of wing cracks in the concrete structure. Defects of this type develop when there is a complex state of stresses in the material and cracks start to develop in the Mode II, e.g. [14 - 16] or Mixed Mode fracture, e.g. [17]. Regarding concrete, the situation is unfavourable, because this is the material of low resistance to shearing and high sensitivity to shear stresses. Fracture toughness under Mode I were presented in [18, 19] but unfortunately, there is a lack of the fracture toughness data K_{IIc}, for concretes containing FA additives. Therefore in this paper we focused on the estimation of the fracture toughness K_{IIc} of the concrete composites modified with FA additives and numerical modelling of crack propagation under Mode II. In order to observe macroscopic crack paths propagation we used of the following equipments: MTS 810 hydraulic press and apparatus for 3D optical analysis of deformations including 3-D Image Correlation System (*3-D ICS*) designed for data recording and processing.
In particular a new 3-dimensional (3-D) numerical model of the *CSS* containing two sharp notches was created using XFEM. It enables observation of defect initiation and development up to the final failure of the concrete. We used peak principal stress criterion for description of the crack grow, taking into account the investigated experimental data concerning strength parameters and fracture energy. The obtained results with the newly formulated 3-D numerical XFEM model coincide with experimental tests very well.

MATERIALS AND PREPARATION

Two concrete mixtures were used for testing of the basic strength of materials characteristics and the fracture toughness are mixtures: without FA additive (FA-00) and with a 20% additive of FA (FA-20). The following materials were used for preparation of concrete mixtures: Portland cement CEM I 32.5 R, natural gravel aggregate of maximum grain size up to 8 mm, pit sand, FA and plasticizer (0.6% of binding material weight). All mixtures had the same water-binding material ratio: w/c+(FA) = 0.4. Composition of the mixtures is specified in Table 1.

Table 1. Composition of the concrete mixtures

Type of concrete	cement (kg/m^3)	fly-ash (kg/m^3)	water (kg/m^3)	pit sand (kg/m^3)	aggregate (kg/m^3)	plastificizer (kg/m^3)
FA-00	352	0	141	676	1205	2
FA-20	282	70	141	676	1205	2

The FA used for the tests was delivered from Puławy thermal-electric power station. According to the guidelines specified in Polish standard [20], this FA was characterized by the following parameters:

- loss on ignition: category A, below 5%,
- fineness: category S, below 12%,
- specific density: 2.1 g/cm^3.

Characteristics of hardened concrete (6 specimens for each tests) with statistic parameters (standard deviation - s and coefficient of variation - ν) are summarized in Table 2.

Table 2. Characteristics of the hardned concrete

Analyzed parameter	Type of concrete	
	FA-00	FA-20
compressive strength on cubes		
f_{cm} (MPa)	47.51	48.96
s (MPa)	2.55	3.02
ν (%)	4.58	7.53
tensile strength by splitting		
f_{ctm} (MPa)	3.58	3.36
s (MPa)	0.13	0.35
ν (%)	4.62	11.6
coefficient of elasticity		
E_{cm} (GPa)	37.27	36.24
s (GPa)	2.25	3.68
ν (%)	4.85	7.54

In the tests to evaluate concrete fracture toughness and crack paths propagation, a method of loading specimens according to the Mode II fracture was used. For the experiments cubes with two sharp notches were used [15]. The target crack sizes were obtained by embedding in concrete the cubes being formed two 4 mm steel sharpened flat bars. Preparation *CSS* were shown in Fig. 1.

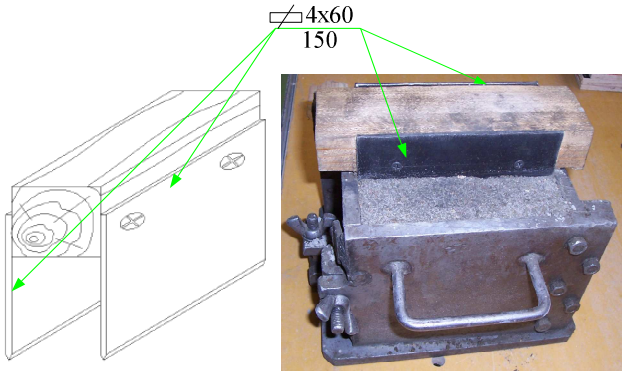

Figure 1. The specimen for Mode II fracture tests during preparation.

EXPERIMENTAL RESEARCH

Purpose and scope of the tests

The principal purpose of the research was to estimate the influence of modification of structural concrete composition with FA additive on basic parameters of fracture mechanics and fracture processes specified for the Mode II of defect development. The tests were performed with the use of the following equipment: MTS 810 hydraulic press equipped with electronic system for measurement data recording and apparatus for 3D optical analysis of deformations including *3-D ICS*, e.g. [21 - 23] designed for data recording and processing. During the tests, the specimens were loaded with a steadily increasing force. The force increase was regulated on the basis of the speed of the press head displacement in the function of time. The displacement value was assumed at the level of 0.25 mm/min. Fracture toughness of the concretes was determined on the basis of analysis of K_{IIc}. K_{IIc} was determined according to the Eq. 1 proposed by J. Watkins [24]:

$$K_{IIc} = \frac{5.11 F_Q}{2Bb}\sqrt{\pi a} \tag{1}$$

where: F_Q - value of critical force corresponding to beginning of the crack growth, b - specimen height above the sharp notch, B - thickness of specimen, a - length of the sharp notch.

Additionally, thanks to the possibility provided by *3-D ICS* system of monitoring the development of the sharp notches in the specimen, the moments of crack initiation as well as important geometric parameters could be observed. The important issues that are implemented later into the numeric models are, e. g., the following: noticing the actual direction of crack propagation and inclination of the cracks with regard to the sharp nothche's plane.

Test results and their analysis

Table 3 summarizes average values of K_{IIc} determined during the tests. Basing on the analysis of the results, one can conclude that FA-20 concrete had 3.5% higher values of K_{IIc} than concrete without FA additives.

Table 3. Average values of the critical stress intensity factor K_{IIc}

Analyzed parameter	Type of concrete	
	FA-00	FA-20
K_{IIc} (MN/m$^{3/2}$)	4.24	4.39
s (MN/m$^{3/2}$)	0.65	0.81
ν (%)	9.43	11.63

NUMERICAL MODELLING CRACK PATHS USING XFEM METHOD

Numerical calculations were made in ABAQUS program, applying XFEM approach, using newly created 3-D model for the *CSS* subjected to shear, e.g. [25 - 28]. Numerical modelling was made for concrete FA-20. The maximum principal stresses criterion was applied in the description of the crack growth, taking into account data gathered during experimental research: concrete strength parameters (Table 2) and fracture energy, e.g. [29]. The dense finite element mesh was created in: the crack area and the central part of the *CSS* (Fig. 2b). Fig. 2a shows the specimen with load configuration, whereas Fig. 2b the applied finite element mesh. The shape of introduced sharp notch used in the numerical model was similar to the shape of sharp notch in the experimental specimens, Fig. 2c. Fig. 3 shows boundary conditions applied in numerical model.

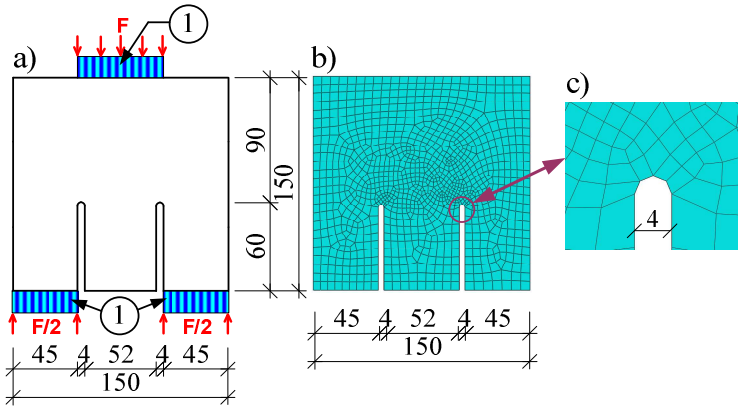

Figure 2. The specimen with: a) load configuration, b) finite elemnt mesh, c) sharp notch; 1- stiff plate.

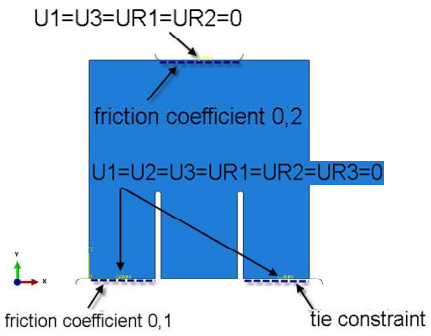

Figure 3. Boundary contitions applied in numerical model: U - dispalcemnt, UR - rotation.

The model consisted of the following three parts: the *CSS*, a stiff plate exerting pressure and 2 stiff supports. One of the supports was treated as non-slidable, while between the second support and the specimen the friction coefficient was assumed to be equal to 0.1. Between the upper stiff plate and the *CSS* the friction coefficient was equal to 0.2. The loading process was controlled by displacement of the stiff plate. The crack always grew in the *CSS* on the side of the non-slidable support. The same manner of cracks propagation was observed in the experimental research. Fig. 4 shows stages of crack development.

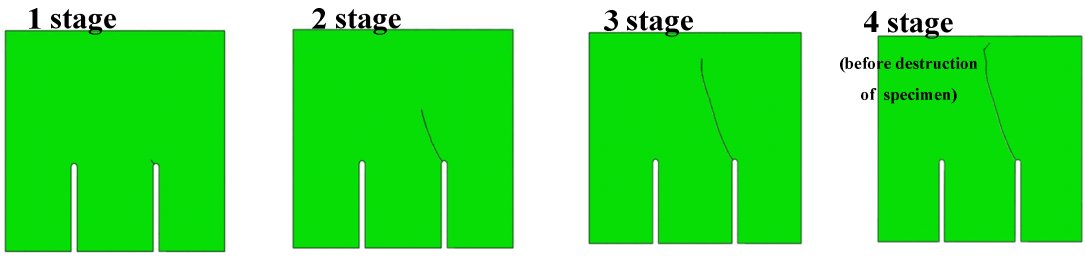

Figure 4. Stages of crack development.

COMPARISON OF CRACK PATHS

The numerical results are consistent with the experimental ones. Convergence of results with regard to the following was observed: shape of cracks (Fig. 5), values of critical force F_Q initiating development of sharp notches, force-displacement diagrams [30].

Fig. 5 shows comparison of shape of cracks obtained during experiments (Fig. 5a and 5b) and numerical simulation (Fig. 5c and 5d). Comparison of the both crack shapes, i.e. from experiment and numerical modelling confirms correctness of assumptions made in the finite element approach.

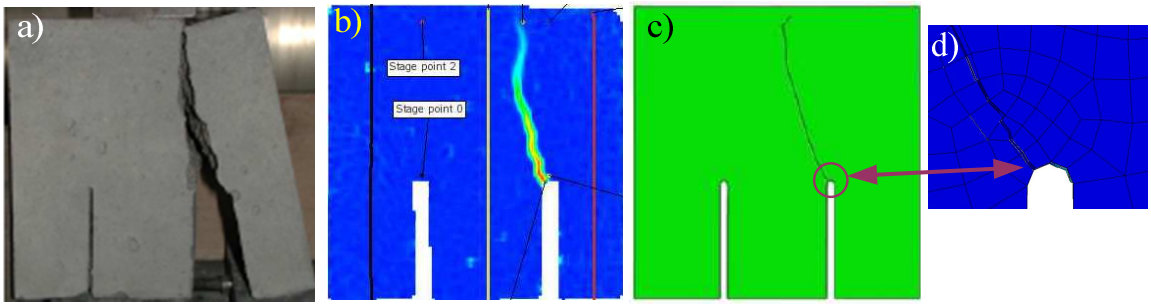

Figure 5. Shapes of cracks obtained: a) during experiment, b) during experiment in *3-D ICS*, c) in ABAQUS numerical simulation, d) crack in sharp notch area.

FINAL REMARKS

The results of experimental part of this paper lead to the main conclusions:

- replacement of 20% of cement with the additive of active pozzolana - siliceous FA increases fracture toughness K_{IIc} in 3,5% of concrete after 28 days of curing,
- crack path was experimentally determined.

The new numerical model for the 3-dimensional *CSS* was created in ABAQUS program in order to describe progressive fracture process of the concrete composite under Mode II (XFEM approach). For cracks propagation the maximum principal stress criterion at the crack tip was applied. The whole crack path, starting from initiation to the specimen failure, was numerically determined.

The following final conclusions can be formulated on the basis of the experimental research and numerical analyses:

- during experiment crack paths were initiated always from the one crack tip, on the side of the non-slidable support,
- the numerical results are convergent qualitatively and quantitatively with the experimental ones, (Fig. 5) [30],
- the model can be extended to more complex specimens geometry and mixed mode cracks propagation under 3-D loading.

It can be stated that analyzing concrete properties and crack paths using the Mode II fracture can be used to assess the durability and safety of the working constructions subjected to shear e.g. analysis: concrete, reinforced concrete and composite concrete beams in the support areas, reinforced concrete wall-beams, reinforced concrete flat slabs.

ACKNOWLEDGEMENT

The research leading to these results has received funding from the European Union Seventh Framework Programme (FP7/2007 – 2013), FP7 - REGPOT – 2009 – 1, under

grant agreement No: 245479; CEMCAST. The support by Polish Ministry of Science and Higher Education - Grant No 1471-1/7.PR UE/2010/7 - is also acknowledged.

REFERENCES

1. Benavidez E., Grasselli C. and Quaranta N. (2003) *Cer. Int.* **29**, 61-68.
2. Oner A., Akyuz S. and Yildiz R. (2005) *Cem. Conc. Res.* **35**, 1165-1171.
3. Raghu Prasad B. K., Eskandari H. and Venkatarama Reddy B. V. (2009) *Cons. Build. Mat.* **23**, 117-128.
4. Gao P. W., Wu S. X., Lin P. H., Wu Z. R. and Tang M. S. (2006) *ACI Mat. J.* **103**, 336-338.
5. Zhang W. M., Ba H. J. and Chen S. J. (2011) *Cons. Build. Mat.* **25**, 2269-2274.
6. Sadowski T. (1994) *Mech. Mat.* **18**, 1-16.
7. Sadowski T. (1994) *Int. J. Dam. Mech.* **3**, 212-233.
8. Sadowski T. (1995) *Int. J. Dam. Mech.* **4**, 293-318.
9. Sadowski T., Samborski S. (2003) *Comp. Mat. Sci.* **28**, 512-517.
10. Sadowski T., Samborski S. (2003) J. Am. Cer. Soc. **86**, 2218-2221.
11. Sadowski T., Postek E. and Dennis C. (2007) *Comp. Mat. Sci.* **39**, 230-236.
12. Sadowski T., Golewski G. (2008) *Comp. Mat. Sci.* **43**, 119-126.
13. Lenci S., Piattoni Q., Clementi F. and Sadowski T. (2011) *Int. J. Frac.* **172**, 193-200.
14. Reihardt H. W., Xu S. (2000) *Int. J. Frac.* **105**, 107-125.
15. Golewski G., Sadowski T. (2006) *Proc. Int. Symp. "Brittle Matrix Composites 8"*, Woodhead Publishing Limited, Warsaw, Poland, 537-546.
16. Rao K. B., Bhaskar Desai V. and Jagan Mohan D. (2012) *Cons. Build. Mat.* **27**, 319-330.
17. Di Prisco M., Ferrara L., Meftah F., Pamin J., De Borst R. and Mazars J. M. (2000) *Int. J. Frac.* **103**, 127-148.
18. Lam L., Wong Y. L. and Poon C. S. (1998) *Cem. Conc. Res.* **28**, 271-283.
19. Tang W. C., Lo T. Y. and Chan W. K. (2008) *Mag. Conc. Res.* **60**, 237-244.
20. PN-EN 450-1 (2009), *Fly ash for concrete. Part 1: Definitions, specifications and category of correspondence*. (In Polish).
21. Caduff D., Van Mier J. G. M. (2010) *Cem Concr. Comp.* **32**, 281-290.
22. Leplay P., Rethore J., Meille S. and Baietto M. C. (2011) *Int. J. Frac.* **171**, 35-50.
23. Wu Z., Rong H., Zheng J., Xu F. and Dong W. (2011) *Eng. Frac. Mech.* **78**, 2978-2990.
24. Watkins J. (1985) *Int. J. Frac.* **23**, R135-R138.
25. Meschke G., Dumstorff P. (2007) *Comp. Meth. Appl. Mech. Eng.* **196**, 2338-2357.
26. Su X., Yang Z. and Liu G. (2010) *Act. Mech. Sol. Sini.* **23**, 271-281.
27. Yu R. C., Ruiz G. and Chaves E. W. V. (2008) *Eng. Frac. Mech.* **75**, 117-127.
28. Xu Y., Yuan H. (2009) *Comp. Mat. Sci.* **46**, 579-585.
29. Ribeiro S., Rodrigues J. A. (2010) *Cer. Int.* **36**, 263-274.
30. Golewski G. L., Sadowski T. (2012) *Sol. Stat. Phenom.* **188**, 158-163.